

¹Payal Ghutke²Wani Patil

IoT Enabled Design of an Analog-front End for the In-vitro Tooth Cavity pH sensor and Testing under Laboratory Conditions



Abstract: - The tooth's pH has an impact on the tooth cavity, which mostly develops as a result of cariogenic bacteria interacting with the carbohydrates in meals. For this purpose, pH sensor has been developed along with the in-house developed analog front end. Developed pH sensor shows change in the resistance when exposed to the tooth's pH. This change in the resistance is measured with the help of a voltage divider circuit followed by a unity gain buffer. Unity gain buffer is used to avoid the loading effect. Further, the output of and buffer is given to the microcontroller and subsequently to an ESP module for Internet of Things (IoT) communication.

Keywords: pH sensor, tooth cavity, analog front-end.

I. INTRODUCTION

The main cause of tooth decay, which is a lack of attention to oral cleanliness, is a fatal situation for teeth, which results in tooth loss [1-2]. When cariogenic bacteria and the carbohydrates on the tooth come into contact, tooth decay begins to develop. This bacteria produces organic acid as a byproduct, which interacts with the tooth and interferes with the balanced tooth restoration mechanism [3-4]. There is a lack of mechanisms for early detection and quick control actions, which would prevent major tooth loss and improve quality of life. The typical testing technique used by dentists today includes visual inspection, and for this purpose, dental explorers are frequently utilised by dentists [5-6]. However, for the visual inspection, a high level of technical knowledge is required; otherwise, the inspection may produce incorrect results. Aside from that, it is critical to develop a strategy for predicting dental cavity diagnoses and providing quantitative data. In addition to the aforementioned procedures, precautions must be taken when utilising dental explorers to avoid infection or fractures [7-9]. As a result, there are few diagnostic techniques for diagnostic tests that are accurate and provide quantitative data when taking into consideration the non-invasive approach of identifying tooth cavities.

Researchers and dentists have investigated the combination of visual inspection with other techniques such as radiographic examination [10-12], pH detection [13-14], and fluorescence [12-15] in order to reduce tooth loss caused by improper cavity prediction. Desist receives the gray-scale image during radiographic inspection, which is mapped to the density loss as a result of mineral content. However, this method has some major drawbacks, including low selectivity and sensitivity, which reduces the accuracy of dental decay detection. Thus, some researchers have reported the use of pH detection and fluorescence-based inspection techniques to improve detection accuracy. Intriguingly, pH detection is chosen above the other two tooth cavity detection techniques partly because it directly correlates with the bacterial activity inside the tooth.

Researchers have reported several types of sensors and electrode systems for pH measurement in the tooth cavity, including the fabrication of antimony electrodes [16-18], pH imaging [19], and ion-sensitive field effect transistors (ISFETs) [20-22]. The primary problem with antimony electrodes is that they produce toxic elements that are harmful to organisms that live. pH imaging dental cavity detection delivers incredibly accurate results, but the main disadvantage is the acquisition device, which is enormous and impractical for patients to use. In earlier published work, where they also used pH imaging devices and linked the data with dental caries, they explained the impact of pH data on the tooth cavity [20]. Researchers designed and fabricated the ISFET for pH sensing using advances in micro-sensor fabrication technology. The main disadvantage of this technique is the high cost of

¹Ph.D. Research Scholar, Department of Electronics & Telecommunication Engineering, G H Raisoni University, Amravati, India

payal.ghutke@raisoni.net

²Assistant Professor, Department of Electronics Engineering, G H Raisoni College of Engineering, Nagpur, India

wani.patil@raisoni.net

fabricating the ISFET, as well as the large amount of data required to comprehend its reliability in clinical trials. Thus, the impetus for designing a low-cost sensor that can detect pH and map the detected pH to the dental cavity. For this purpose, we have fabricated the pH sensor to detect the tooth cavity, which is reported in our earlier work [28]. However, for the ease of use and to provide the accurate control measures analog front end plays a pivotal role. Thus, in this work we have explored the analog front end designed for the tooth cavity pH sensor.

II. MATERIALS AND METHODS

2.1 pH sensor for tooth cavity measurement

The fabrication of the pH sensor used in this work has been reported in our earlier work [28]. Our study explored the PH value of the tooth is highly correlated with the tooth cavity. Fig. 1 (a) shows that first we have fabricated the IDEs on the PCB and rGO is drop casted on it. Then the fabricated sensor is exposed to different pH solution ranging from 4 to 12. Sensor transfer characteristics viz. sensitivity, response time, accuracy, etc. has been tested the sensor under laboratory conditions reported in our earlier work [28].

Fig. 1 (b) shows that rGO is utilised as the sensing film that is drop casted on the fabricated sensor during measurements, and it is covering the entire surface area of the sensor. Further, we have observed that fabricated sensor resistance increases with increase in the pH values as discussed in the previous paper [28]. Further we have analysed the sensor's change in resistance with the help of Keithley multi-meter (DMM 6500) when exposed to various pH sample ranging from 4 to 12 as depicted in Fig. 1 (b)

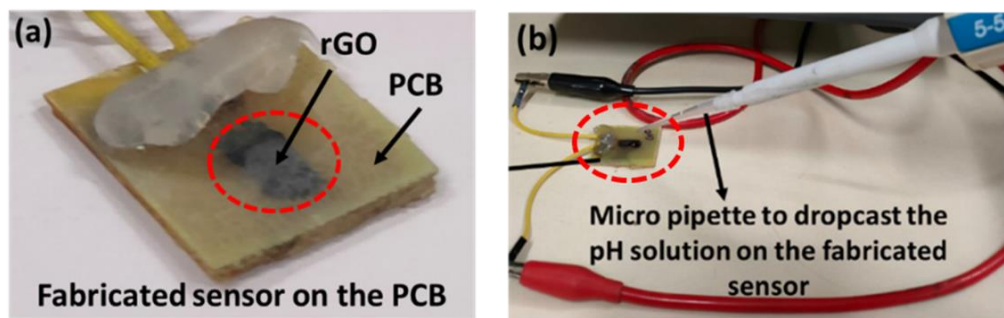


Figure. 1 (a) fabricated sensor and (b) experimental set-up used for the lab testing

2.2 Developed hardware

Fig. 2 (a) shows the process flow chart of the system design and testing protocol. For this process first, the designs of the circuit were made in three main sections i.e. power supply voltage, micro-controller voltage and sensor output voltage. Before starting the measurements, it has to be ensured that all the section should get the desired voltage and the current levels for proper operation. Once it is done then only we will get the desired voltage values from all the modules. Fig. 2 (b) represent the block diagram of the system on the printed circuit board (PCB). For using system board testing, we have divided the board into three sections: (i) the power supply section, (ii) the IC voltage section, and (iii) the sensor output section. This section. The power supply section ensures to deliver the required power to the entire system, which comprise of sensor, analog front end, and microcontroller and Wi-Fi module.

Further, we have used the battery for power section area, power supply section has been designed to power the complete system as shown in Fig. 2 (b) first block area i.e. Li-ion battery rated at 4.2V, 2200 mAh capacity is used. Power supply voltage regulators are requisite for providing a regulated voltage to the entire system. During measurements we have monitored the battery voltage to testing the circuit board. We have used microcontroller At-mega 328, IC voltage regulator, resistive-based pH sensor, which is interfaced with the developed hardware. As depicted in Fig. 2 (b), each block sequentially followed the testing protocol.

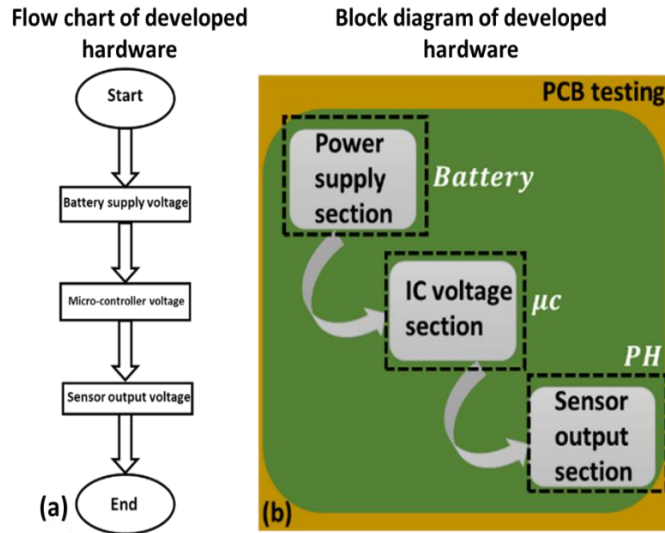


Figure 2: Flow chart for testing of the developed hardware, (b) block diagram for the proposed hardware

Fig. 3 (a) shows the schematic circuit, which is designed in the EAGLE software. It comprise of four major sections viz (i) main power section to gives the supply voltage to the system, (ii) ESP8266 Wi-Fi module is included, which is used to send data on the server, (iii) microcontroller to control the system and manage the sensor output data and (iv) voltage divider circuit. Power supply section generates the 3.3 V and microcontroller unit takes the data from voltage divider circuit and then that value will be transferred to the server with the help of Wi-Fi module. Fig. 2(b) shows a layout design of the circuit, which shows the routing information of the schematic.

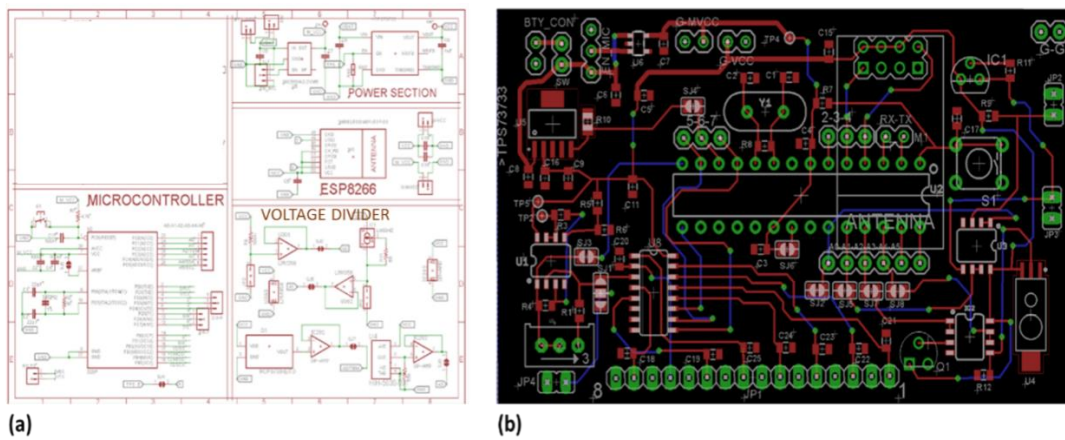


Figure. 3 (a) shows the actual schematic circuit and (b) board made using the Eagle software.

III. RESULTS AND DISCUSSION

3.1 Simulation

It is important to validate the relation between the change in resistance of the sensor due to pH and output voltage of the developed hardware with the help of simulation. For this purpose, we have used the TINA-TI software, where voltage divider circuit followed by an unity gain buffer is used. Fig. 4 shows the simulation results achieved using the TINA TI for various resistance (for corresponding pH values) and their respective voltage values. From Fig. 4 (a), it is evident that, we have fixed the value of resistance 26 KΩ (corresponding to pH 12) then by using developed hardware, which comprise of voltage divider followed by buffer generated 2.71 V at the output. Similarly, as shown in Fig. 4 (b), we changed the resistor value 22.4 KΩ (corresponding to pH value 9) then at the output 2.52V has been observed. Further as depicted in Fig. 4 (c) when resistance is 22 KΩ (corresponding PH value is 7) then the circuit generates 2.50 V at output. Likewise, as depicted in Fig. 5 (d) when sensor resistance is 21.8 K ohms (corresponding pH value is 4) then the circuit generates 2.49 voltage at output.

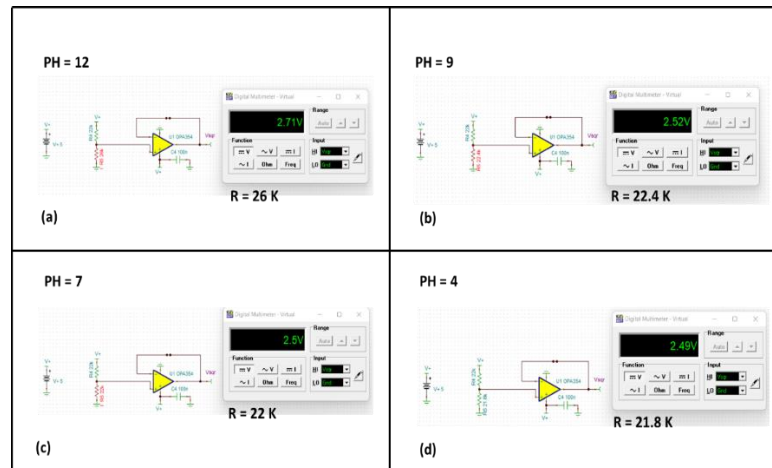


Figure 4: Simulation result for the proposed hardware

3.2 Lab testing

Fig. 5 shows the testing of the different section areas, viz battery voltage, regulator IC voltage and output voltage of the voltage divider circuit (when fabricated sensor is connected). Fig. 5 (a) shows the battery voltage in the multi-meter. Further, the battery is connected to the regulator is, which is designed to generate 3.3 V. As depicted in Fig. 5 (b) voltage regulator generates 3.24 V, which shows the absolute error of the voltage regulator is about 60 mV less. Further, Fig. 5 (c) shows the voltage divider circuit output when fabricated pH sensor is connected to it. For this purpose, we have first dropcasted the pH on the fabricated sensor ensuring that entire sensor area is covered with the pH sample and corresponding voltage is measured with the help of a digital multimeter. It has been observed that with decrease in the pH value, the voltage of the circuit decreases, which is attributed to the decrease in the resistance of the sensor.

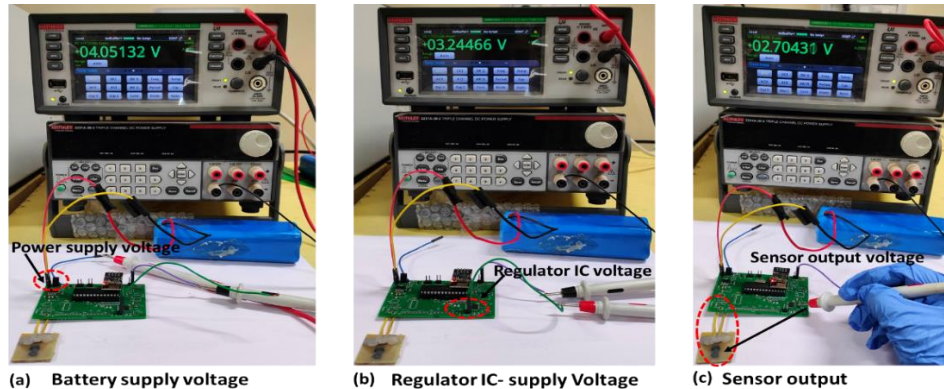


Figure 5: Testing of the developed hardware, (a) battery voltage, (b) output voltage of the regulator IC and (c) voltage divider circuit output when pH is dropcasted on the fabricated sensor.

By using the experimental set-up described in section 3.2, it has been observed that the fabricated pH sensor voltage value increases with an increase in the pH samples coverage on sensing areas. Further, from Fig. 6 (a) it is evident that if the resistance changes when exposed to pH values from ranges (4 to 12) the voltage of the circuit increase. Thus, our experimental results show that with increase in the pH value (ranging from 4 to 12), then voltage value increases, which is in agreement with the simulation results as described in section 3.1.

Further, it is very important that the measured voltage using the developed hardware needs to be accurate in order to avoid error in the measurement systems. For this purpose, we have measured the voltage using developed hardware and benchmarked with the Keithley digital multimeter (DMM6500). Fig. 6 (b) shows the benchmarking of the measured voltages using Keithley multimeter with developed hardware. From Fig. (b) it is evident that measured voltage between developed hardware follows linearly with the DMM6500. Further, the main objective of the analog front end is to measure the resistance of the sensor which is related to the pH (as shown in Fig. 6.1) with minimal error. Thus, to analyse the measured resistance measured using developed

hardware and benchmark with the Keithley digital multimeter (DMM6500), we have connected the standard resistor in the voltage divider circuit and also the value of the standard resistor is measured using the Keithley digital multimeter (DMM6500). Fig. 6 (c) depicted that the measured resistance value using multimeter with developed hardware, which ensured the good linearity between both the methods used for the resistance measurements.

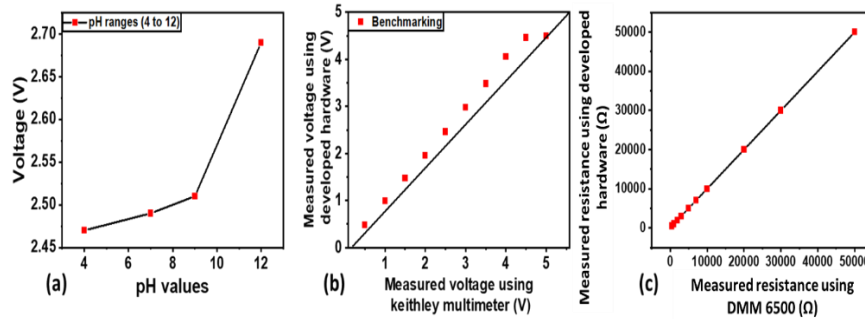


Figure 6: (a) relation between the measured voltage using the developed hardware and pH values, (b) benchmarking of the measured voltage using Keithley digital multimeter (DMM6500) and developed hardware, (c) benchmarking of the measured resistance using Keithley digital multimeter (DMM6500) and developed hardware.

3.3 IOT Data transmission to Matlab

The proposed analog design circuit as mentioned above converts the change in resistance to voltage and microcontroller is used for data acquisition. As shown in Fig.3.a ESP8266 Wi-Fi module is connected to a microcontroller via UART interface which is also called as transmitting module. Similar receiver Wi-Fi module is connected to a laptop, and it is responsible to collect all the data from transmitter module and send it to Matlab Wi-Fi ThingSpeak [27]. ThingSpeak is inbuilt Matlab API to process real-time data and the data received to Matlab's wifi ThingSpeak is used for data visualization and to publish data of the transmitter module hardware to the Internet of Things.

3.4 PCA and K-Mean Clustering

The data collected from Matlab's ThingSpeak is used for further analysis and given to PCA and K-mean algorithm. PCA cluster the PH data based on the changed in resistance value and K-mean classify the PH-data and describe whether tooth cavity is present or not. As shown in Fig. 8 (a) shows the PCA and k-mean results of the data that is collected from the developed hardware. As explained in previous section rGO sensor has been tested with proposed hardware circuit for 4 different Ph values i.e. 4, 7.5, 9 and 12 respectively. Sensor response to different Ph value with different pattern and these patterns given to PCA and K-Mean classifier and it is observed that all Ph values are separated out properly. Total 40 experiments were performed with rGO sensor to create Training data sets. And for testing two Ph Sample were taken i.e. 7.5 and 12. When PH 7.5 sample was given as test sample it was able to properly classify with PH-7.5 group. Similarly, When PH 12 sample was given as test sample it was able to properly classify with PH-12 group.

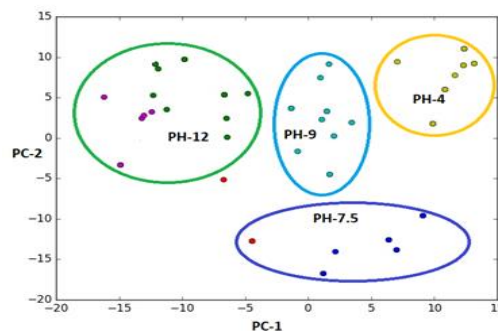


Figure 8: PCA and K-Mean cluster data for different PH values representing tooth cavity.

IV. CONCLUSION

In this paper a cost effective, portable, and affordable IoT enabled tooth cavity system is developed and demonstrated. It has rGO based resistive sensors as a main component to measure the PH value by changing its resistance and it is measured by proposed analog front-end circuit. The front-end analog circuit convert the change in resistance to voltage and this change is measured by microcontroller. Microcontroller measure this change in voltage via ADC and transfer the measured data to Matlab's ThinkSpeak via Wi-Fi Module. The data collected by Matlab ThinkSpeak is further processed by PCA and K-Mean which is used for the tooth cavity detection.

REFERENCES

- [1] Poul Erik Petersen, Denis Bourgeois, Hiroshi Ogawa, Saskia Estupinan-Day, Charlotte Ndiaye (2005), "The global burden of oral diseases and risks to oral health," *Bulletin of the world health organization*, vol. 83, pp. 661-669.
- [2] Pitts, Nigel B., "et al." (2017), "Dental caries," *Nature reviews Disease primers*, vol. 3.1 pp. 1-16.
- [3] A F Paes Leme, H Koo, C M Bellato, G Bedi, J A Cury (2006), "The role of sucrose in cariogenic dental biofilm formation—new insight," *Journal of dental research*, vol. 85, pp. 878-887.
- [4] Selwitz, Robert H., Amid I. Ismail, and Nigel B. Pitts (2007), "Dental caries", *The Lancet*, vol. 369, pp. 51-59.
- [5] Pitts, Nigel B. (2001), "Clinical diagnosis of dental caries: a European perspective," *Journal of Dental Education* vol. 65 pp. 972-978,
- [6] Ismail, A. I. J. (2004), "Visual and visuo-tactile detection of dental caries," vol. 83, pp. 56-66.
- [7] Ekstrand, Kim, V. Qvist, and A. Thylstrup (1987), "Light microscope study of the effect of probing in occlusal surfaces," *Caries research*, vol. 21, pp. 368-374.
- [8] K W Neuhaus, R Ellwood, A Lussi, N B Pitts (2009), "Traditional lesion detection aids," *Detection, assessment, diagnosis and monitoring of caries*, vol. 21, pp. 42-51.
- [9] Juliana Mattos-Silveira, Marina Monreal Oliveira, Ronilza Matos, Cacio Moura-Netto, Fausto Medeiros Mendes, and Mariana Minatel Braga (2016), "Do the ball-ended probe cause less damage than sharp explorers?—An ultrastructural analysis," *BMC oral health*, vol. 16, pp. 1-7.
- [10] D N Ricketts, E A Kidd, B G Smith, R F Wilson (1995), "Clinical and radiographic diagnosis of occlusal caries: a study in vitro," *Journal of Oral Rehabilitation*, vol. 22, pp. 15-20.
- [11] Wenzel, A. (1998), "Digital radiography and caries diagnosis," *Dentomaxillofacial Radiology*, vol. 27, pp. 3-11.
- [12] Pretty, Iain A. (2006), "Caries detection and diagnosis: novel technologies," *Journal of dentistry*, vol. 34, pp. 727-739.
- [13] Igarashi, K., I. K. Lee, and C. F. Schachtele (1989), "Comparison of in vivo human dental plaque pH changes within artificial fissures and at interproximal sites," *Caries research*, vol. 23, pp. 417-422.
- [14] A Smit, M Pollard, P Cleaton-Jones, A Preston (1997), "A comparison of three electrodes for the measurement of pH in small volumes," *Caries research*, vol. 31, pp. 55-59.
- [15] A Lussi, S Imwinkelried, N Pitts, C Longbottom, E Reich (1999), "Performance and reproducibility of a laser fluorescence system for detection of occlusal caries in vitro," *Caries research*, vol. 33, pp. 261-266.
- [16] Gen Mayanagi, Koei Igarashi, Jumpei Washio, Nobuhiro Takahashi (2017), "pH response and tooth surface solubility at the tooth/bacteria interface," *Caries research*, vol. 51.2, pp. 160-166.
- [17] Thompson, F. Clarence, and Finn Brudevold (1954), "A micro-antimony electrode designed for intraoral pH measurements in man and small experimental animals," *Journal of Dental Research*, vol. 33.6, pp. 849-853
- [18] I Kleinberg, G N Jenkins, R Chatterjee, L Wijeyeweera (1982), "The antimony pH electrode and its role in the assessment and interpretation of dental plaque pH," *Journal of Dental Research*, vol. 61, pp. 1139-1147.
- [19] Noriko Hiraishi, Yuichi Kitasako, Toru Nikaido, Satoshi Nomura, Michael F Burrow, Junji Tagami (2003), "Effect of artificial saliva contamination on pH value change and dentin bond strength", *Dental Materials*, vol. 19, pp. 429-434.
- [20] Keiko Murakami, Yuichi Kitasako, Michael F Burrow, Junji Tagami (2006), "In vitro pH analysis of active and arrested dentinal caries in extracted human teeth using a micro pH sensor," *Dental materials journal*, vol. 25, pp. 423-429
- [21] Yuichi Kitasako, Nathan J Cochrane, Matin Khairul, Kanako Shida, Geoffrey G Adams, Michael F Burrow, Eric C Reynolds, Junji Tagami (2010), "The clinical application of surface pH measurements to longitudinally assess white spot enamel lesions," *Journal of dentistry*, vol. 38, pp. 584-590
- [22] Mie Fujii, Yuichi Kitasako, Alireza Sadr, Junji Tagami (2011), "Roughness and pH changes of enamel surface induced by soft drinks in vitro-applications of stylus profilometry, focus variation 3D scanning microscopy and micro pH sensor," *Dental materials journal*, vol. 30, pp. 404-410.
- [23] Patle, Kamlesh S., Hemen K. Kalita, and Vinay S. Palaparthi (2022), "Reduced Graphene Oxide Soil Moisture Sensor with Improved Stability and Testing on Vadose Zone Soils," *Artificial Intelligence Driven Circuits and Systems*. Springer, Singapore, pp. 115-123.
- [24] Chindanai Ratanaporncharoen, Miyuki Tabata, Yuichi Kitasako, Masaomi Ikeda, Tatsuro Goda, Akira Matsumoto, Junji Tagami, Yuji Miyahara (2018), "pH mapping on tooth surfaces for quantitative caries diagnosis using micro Ir/IrOx pH sensor," *Analytical chemistry*, vol. 90 pp. 4925-4931.

- [25] Cooper, R., & Harrison, A. (2009). The exposure to and health effects of antimony. *Indian Journal of Occupational and Environmental Medicine*, 13(1), 3.
- [26] Wang, M., Yao, S., & Madou, M. (2002). A long-term stable iridium oxide pH electrode. *Sensors and Actuators B: Chemical*, 81(2-3), 313–315.
- [27] <https://www.mathworks.com/help/supportpkg/arduino/ref/wifithingspeakwrite.html>
- [28] Ghutke, P. & Patil, W.(2024). In-Vitro Detection of Tooth Decay Using Reduced Graphene Oxide (rGO) based Sensor. *International Journal of Intelligent Systems and Applications in Engineering*, 12(17s), 177–183.